Anal. Bioanal. Electrochem., Vol. 10, No. 8, 2018, 991-1003

Analytical & Bioanalytical Electrochemistry

www.abechem.com

Full Paper

Saccharide Capped Superparamagnetic Metal-ion Doped Iron Oxide Nanoparticles: A Facile Electrochemical Approach to Production

Isa Karimzadeh[1,*] and Ramin Cheraghali[2]

[1]*Department of Physics, Faculty of Science, Central Tehran Branch, Islamic Azad University, Tehran, Iran*

[2]*Department of Chemistry, Saveh Branch, Islamic Azad University, Saveh, Iran*

*Corresponding Author, Tel.: +98-21-44356639; Fax: +98-21-44356639

E-Mail: isa.karimzadeh@gmail.com

Received: 10 January 2018 / Received in revised form: 29 March 2018 / Accepted: 12 June 2018 / Published online: 31 August 2018

Abstract- Here we describe a simple and novel electrochemical synthesis for preparation of Mn doped iron oxide nanoparticles (MIOs) and their surface coating with saccharides (i.e. glucose, sucrose and starch). The electrochemical preparation of MIOs samples were carried out in a two-electrode electrochemical set up including graphite anode and stainless steel cathode. The surface coating with saccharide agents was also performed in the same set up and simultaneously with the formation of iron oxide particles on the cathode surface. The fabricated MIOs were specified through FT-IR, FE-SEM, XRD, DSC-TGA, and VSM analyses. The structural data obtained by XRD proved the magnetite (Fe3O4) crystal phase of samples, and FT-IR and TG data showed the Mn doping and saccharide coat on the surface of the deposited MIONs. The FE-SEM observations and EDS data confirmed the particle morphology and magnetite chemical composition as well as Mn ions doping into the MIONs. The superparamagnetic nature and suitable magnetic ability (i.e. high saturation magnetization, negligible remanent magnetization and coercivity) for the fabricated MIONs were also assessed though vibrating sample magnetometer (VSM) results. These characters of the electrosynthesized sample provided their suitability for biomedical applications.

Keywords- Iron oxide, Nanoparticles, Electrochemical synthesis, Saccharide coating, Magnetization

1. INTRODUCTION

Magnetic nanoparticles (MNPs) have been recently emerged as new cases for application in various nano-medicinal areas due to their unique and important nanoscale physico-chemical capabilities [1-3]. Among MNPs, iron oxide nanoparticles (IONs) have received great consideration in diverse biomedical fields as a result of good colloidal, stability after capping with suitable agents, high relaxation nature, excellent in vivo biocompatibility, and tunable further functionalization [4-7]. IONs, with presenting the unique mechanical, physical, chemical, and thermal abilities, have found amazing fairs in nano/bio-medicinal applications like magnetic resonance imaging [8-10], stem cell tracking [11], hyperthermia [12], gene therapy [13] and cell manipulation [14], and new therapeutic possibilities such as phototherapeutic [15-17] or gene therapeutic agents [18-21], imaging-guided cancer therapy [22-25]. It has been reported that without surface coating with suitable agents, IONs are easily undergo oxidation even at RT condition, leading up reduction of both magnetization and colloidal stability [26]. Notably, colloidal stability and magnetization of iron oxide NPs are important effective factors in their applications of magnetic targeting, magnetic resonance imaging (MRI), and magnetic hyperthermia [27]. Furthermore, IONs tend to be agglomerated as a result of their strong inherent magnetic dipole interactions and high specific surface area (SSA) versus respective volume i.e. surface-to-volume ratio [28,29]. To prevent IONs agglomeration and so high colloidal stability, the design of novel synthesis routs and surface engineering of IONs with appropriate coatings are goal of many researches. Capping or grafting layer formation onto IONs can be constructed using various bio-compatible inorganic or organic materials like as inorganic layers of silver, silica, gold, etc. [30,31], polymers (e.g. chitosan [32], polyvinylpyrrolidone [33,34], polyethyleneimine [35], and polyethylene glycol [36,37]), and organic compounds of oleic acid and amino acids [38], alkyl phosphonates [39]. For fabricating the IONs, electrochemical synthesis, as an alternative procedure, has been reported to be an efficient synthesis method of iron oxide nanoparticles in both naked and coated forms [40-43]. It has been also established that various nanostructures metal oxides could be easily fabricated through cathodic electrochemical deposition (CED) at mild conditions [44-51]. Notably, beside electrochemical strategy, the main chemical techniques including co-precipitation, microemulsion, thermal decomposition, sol–gel, hydrothermal and solvothermal methods have been used to fabricate high-quality/biocompatible Fe_3O_4 NPs [52-54]. Importantly, these chemical/electrochemical methods can be used to prepare steady and size controlled NPs when compared to other physical methods including gas phase deposition and electron beam lithography. Very recently, metal ion doped iron oxide NPs (M=Sm, Gd, La, Zn and Ho) have been synthesized through one-pot CED procedure [55-60]. Here, we applied similar CED procedure for producing the Mn^{2+} ion doped iron oxides (MIONs) and then in situ surface coating with saccharide coating agents (i.e. glucose, sucrose and starch). The

resulting capped MIONs were investigated using XRD, FT-IR, DSC-TGA, FE-SEM and VSM analyses, and the results established the successful production of saccharide caped Mn doped IONs through applied CED strategy.

2. EXPERIMENTAL PROCEDURE

2.1. Materials

The high purity initial chemicals from Sigma-Aldrich chemical company were purchased and used as received: $FeCl_2$.$4H_2O$, $Fe(NO_3)_3$.$6H_2O$, ethanol (99.9%), glucose ($C_6H_{12}O_6$ Mw=180.16), sucrose ($C_{12}H_{22}O_{11,}$ Mw=342.3) and starch($[C_6H_{10}O_5]n$). The graphite plate and stainless steel substrate (316L) were also provided from local companies.

2.2. Electrosynthesis experiments

An aqueous solution of 0.8 g iron(II) chloride and 1.6 g iron(III) nitrate were dissolved in 500 cc distilled water. Then, 0.2 g saccharide coating agent (i.e. glucose/ sucrose/ or starch) was added into the above solution and stirred with magnet for 1 h. The resulting solution was used as the electrolyte in the electrochemical synthesis experiments. Two electrodes of stainless-steel cathode and graphite anode were connected to a DC power supply (PROVA 8000), and used as electrochemical set-up. The electrodeposition experiments were handled in a galvanostatic regime at a current density of 5 mA cm^{-2} for 25 min. At the end of each run, a black deposit was formed on the cathode surface. After each deposition run, the following steps was carried out; (a) The cathodes were removed from the electrolyte and washed several times with distilled H_2O, (b) the black films were scraped from the cathodes and dissolved in an EtOH solution, and (c) the powder washed with ethanol several times to remove free and non-attached saccharides from the IONs surfaces, (d) the powder were then dispersed in EtOH and centrifuged at 6000 rpm for 5 min, and (e) the black powders were separated from the ethanol solutions with magnet and dried in a vacuum oven (70 ^oC for 1h). The powders prepared from the glucose, sucrose and starch dissolved electrolytes were referred to as glucose-MIONs, sucrose-MIONs and starch-MIONs, respectively. The samples were characterized by various structural analysis techniques.

2.3. Sample characterization

X-ray powder diffraction (XRD) analysis was conducted on a Phillips PW-1800 diffractometer Smart Lab operated at 40 kV and 35 mA using with Co Kα radiation (λ=1.789 Å). The thermal stability was determined by thermogravimetric analysis (TGA, PerkinElmer Instruments model, STA 1500). The TGA thermograms were recorded for 5 mg of powder sample at a heating rate of 10 C/min in the temperature range of 30-500 ^oC under nitrogen

atmosphere. The surface morphology of the prepared IONs samples was observed by field-emission scanning electron microscopy (FE-SEM, Mira 3-XMU with accelerating voltage of 100 kV). Fourier transform infrared (FT-IR) spectra were recorded in transmission mode with a Bruker Vector 22 Fourier transformed infrared spectrometer. The powder samples were ground with KBr and compressed into a pellet. FT-IR spectra in the range 4000-400 cm^{-1} were recorded in order to investigate the nature of the chemical bonds formed. The magnetic properties of the samples were studied by Vibrating Sample Magnetometers (VSM) Lakeshore 7410 at room temperature with recording the hysteresis loops from −20000 to 20000 Oe.

3. RESULTS AND DISCUSSION

3.1. Crystal structure

The typical powder X-ray diffraction patterns of the glucose-MIONs, sucrose-MIONs and starch-MIONs are shown in Fig. 1. All the peaks of XRD patterns were compared and easily matched with magnetite standard card i.e. JCPDS No.85-1436 [38]. The samples exhibited very broad peaks indicating the fine and small crystallite size of particles. In all patterns, the strongest reflection peaks from (311) planes are the characteristic of cubic spinel phase of iron oxide [41,44]. The other peaks indexed as (220), (311), (400), (333) and (440) planes relate also to a cubical ones [39].

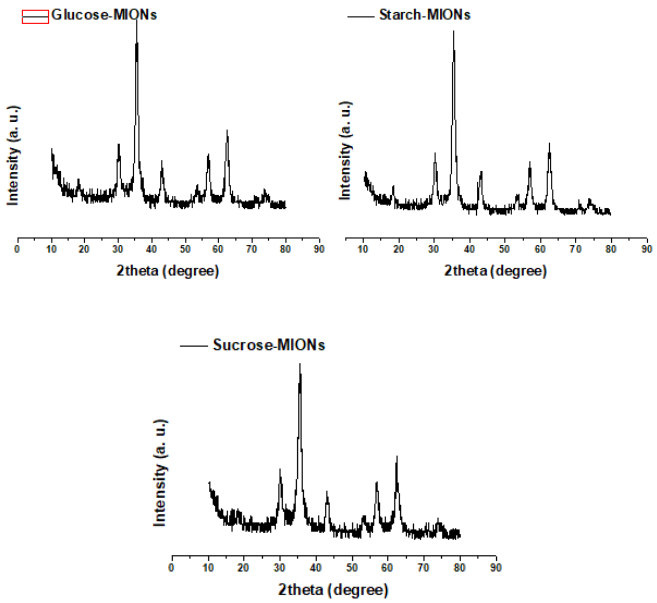

Fig. 1. XRD patterns of the electrosynthesized saccharide capped iron oxide samples

The average crystallite size of nanoparticles could be estimated using Debye Scherrer formula $D=k\lambda/\beta\cos\theta$, where D is the crystallite mean size, k is a shape function for which a

value of 0.9 is normally used, λ is the wavelength of the radiation, β is the full width at half-maximum (FWHM) in the 2θ scale and θ is the Bragg angle [45,52]. It was calculated that the average crystallite sizes of glucose-MIONs, sucrose-MIONs and starch-MIONs to be 7.8 nm, 9.8 nm and 7.4 nm, respectively.

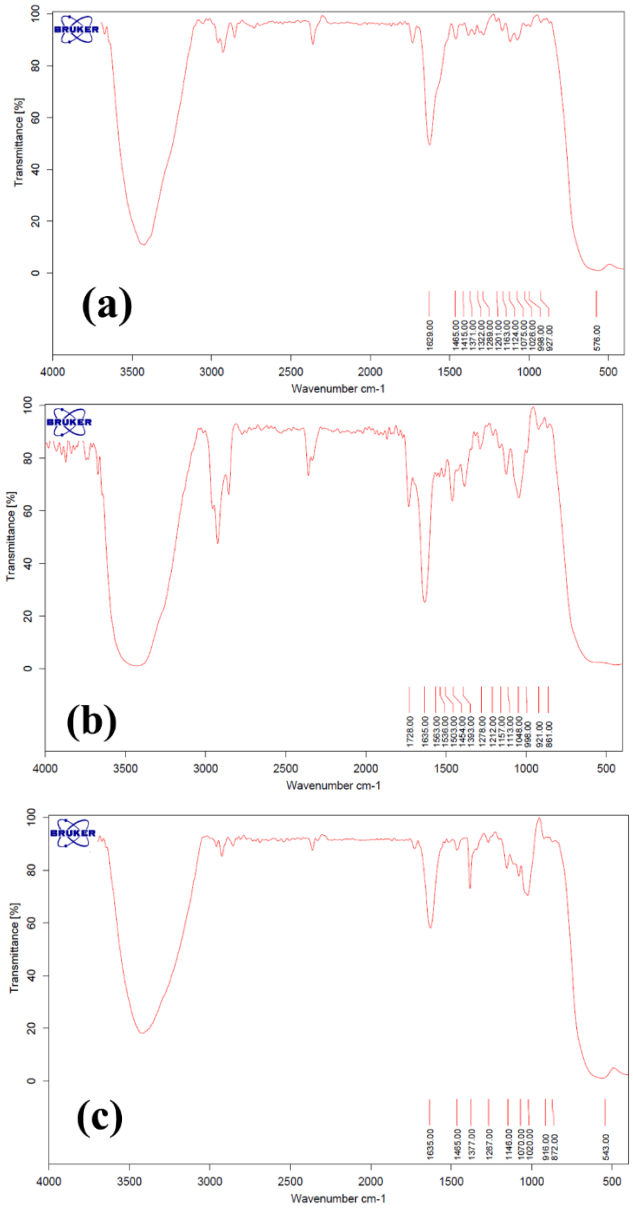

Fig. 2. IR spectrum of the electrodeposited (a) glucose-MIONs; (b) sucrose-MIONs and (c) starch-MIONs samples

3.2. FT-IR

The chemical composition of MIONs and presence of saccharide layer onto the MIONs surface were investigated through FTIR analysis. Fig. 2 presents the IR spectra of the three

electro-deposited MION samples. In all spectra in Fig. 3, the IR bonds below 600 cm^{-1} are related to the Fe-O-Fe and Fe-O-Mn stretching modes [58,61] and also the bands at about 3450 $cm^{-1}$and 1650 cm^{-1} due to the stretching and deformation vibrations of OH groups attached to the surface of MIONs [55,56].

For the glucose capped MIONs, IR spectra presented in Fig. 2a have the following absorption bands: CH_2 asymmetric stretching at 2933 cm^{-1}, CH_2 symmetric stretching at 2858 cm^{-1}, CH_2 scissoring, wagging and twisting at 1465 cm^{-1}, 1371 $cm^{-1}$and 1322 cm^{-1}, respectively, C-O-C stretching at 998 cm^{-1} [62-65], C–O stretching of the C–O–H group at 1289 cm^{-1} and C–O ether bond of the glucose ring at 1026 cm^{-1} [62,64]. These IR data clearly confirmed the successful surface capping of MIONs with glucose molecules through our designed electrochemical strategy.

About the sucrose-MIONs sample, the IR spectrum in Fig. 2b has the IR bands of CH_2 asymmetric stretching, CH_2 symmetric stretching, CH_2 scissoring, CH_2 wagging, CH_2 twisting at the wavenumbers of 2936 cm^{-1}, 2884 cm^{-1}, 1503 cm^{-1}, 1393 cm^{-1} and 909 cm^{-1}, respectively [65-67]. Also, C–O stretching and C–O ether bond at 1048cm^{-1} and 998 cm^{-1} are observed [68]. These data revealed the sucrose coat of the surface of electrochemically fabricated MIONs.

In spectra of starch capped MIONs (Fig. 2c), the IR peaks at 1465, 1377 and 1267 cm^{-1} are related to the CH_2 scissoring, CH_2 wagging and twisting CH_2, respectively [65-67]. CH_2 asymmetric and CH_2 symmetric stretching modes are located at 2932 and 2856 cm^{-1}, respectively [66]. The sharp band at 1020 cm^{-1} is also verified the C–O stretching od starch [66,67]. Hence, IR spectra of starch-MIONs shows all IR bands related to sucrose chemical structure.

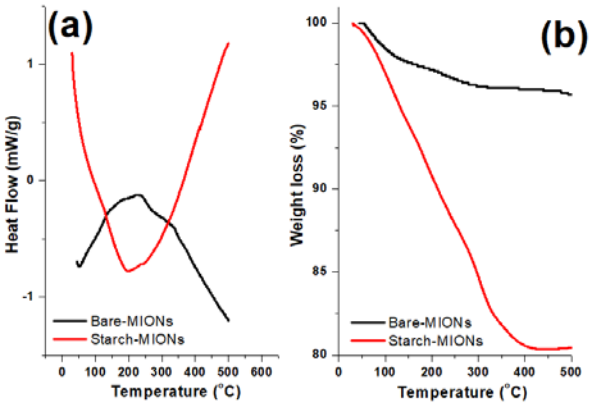

Fig. 3. (a) DSC and (b) related TG curves of the electro-synthesized naked and starch caped iron oxides

3.3. Thermogravimetric (DCS-TG) analyses

Fig. 3 presents the DSC-TG curves for the fabricated starch-MIONs and naked MIONs. For the naked sample, DSC has one endothermic peak at low temperatures (Fig. 3a), which is

due to the removal of attached water molecule on to the oxide NPs [63]. TG curve shows a total weight loss of 3.1% for the naked MIONs (Fig. 3b). The DSC profiles of the starch-MIONs exhibits a-two step sharp endothermic peak at temperatures of 70-400 ^{o}C (Fig. 3a). At low temperatures, this peak is due to the removal of water molecules [64].

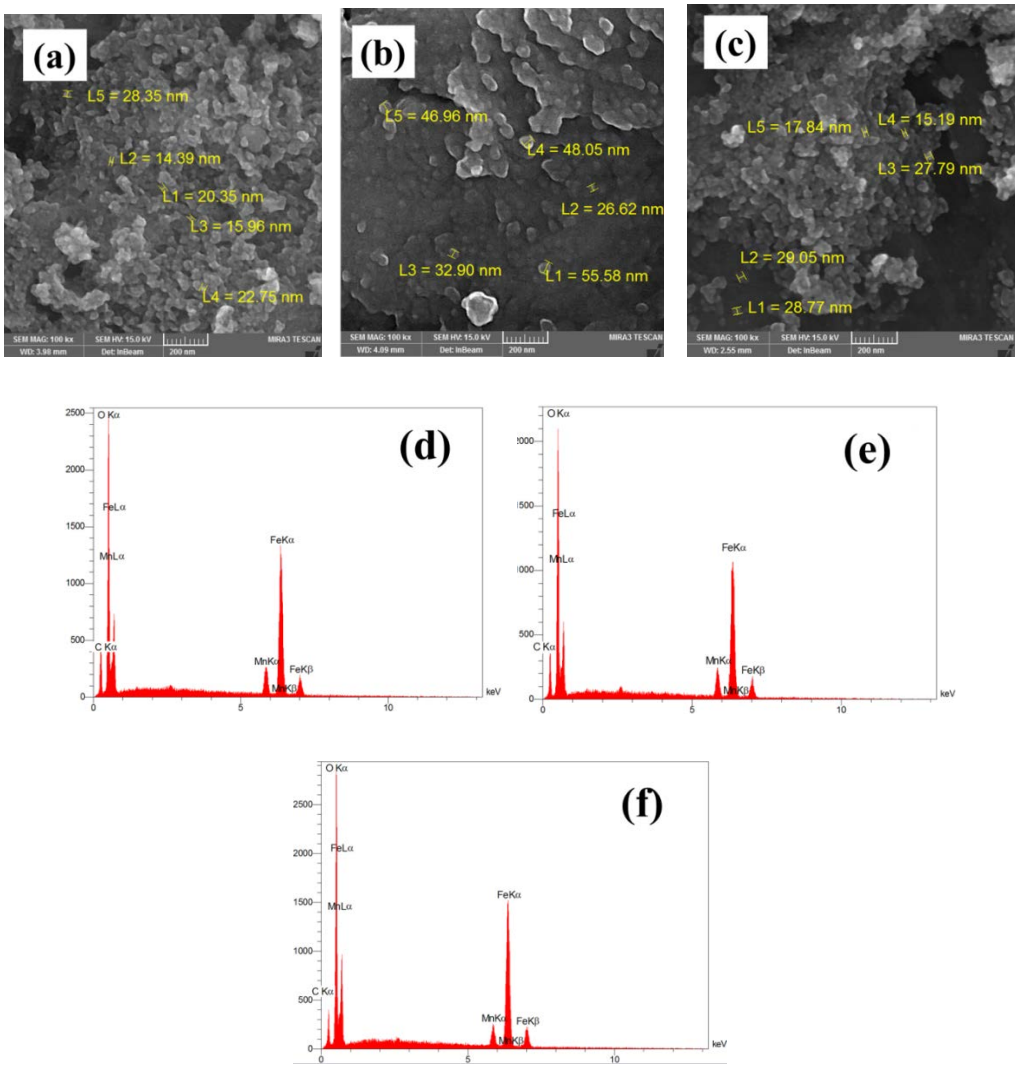

Fig. 4. FE-SEM images and EDS data for the prepared (a,d) glucose-MIONs; (b,e) sucrose-MIONs and (c,f) Starch-MIONs samples

As reported in the literature, the main decomposition of saccharides is occurred at temperatures of 150-400 ^{o}C [66,69], and hence the weight loss observed at the temperature range is due to the decomposition of starch skeleton and its removal from the sample [66,6]. The total weight loss for starch-MIONs is about 28.5%, as seen in Fig. 3b. The increased weight loss of starch grafted sample as compared with those of naked MIONs confirmed the starch layer on the surface of the fabricated MIONs.

3.4. Morphological characterization

The FE-SEM observations and the related energy dispersive spectroscopy (EDS) data of the synthesized sample are presented in Fig. 4. The particle morphologies with relative spherical shapes are observed for all samples (Fig. 4a-c). The glucose capped MIONs have average particle size of 20 nm (Fig. 4a). For the sucrose and starch grafted MNPs, the size of the observed particles are about 30 nm and 25 nm, respectively (Figs. 4c and d). Figs. 3d-f presents the elemental analysis data for the samples. For all three samples, the presence of Fe, Mn and O elements confirmed their Mn^{2+} doped Fe_3O_4 chemical structure. Also, the carbon content in these samples proved the saccharide coat layer on the MIONs.

3.5. Magnetic analysis

To investigate the magnetic properties of the MIONs, we applied the VSM technique, recording hysteresis loops at a magnetic field in the range −20000 to +20000 G at room temperature. As seen in Figure 5, the completely reversible hysteresis loop indicates the superparamagnetic property of the nanoparticles. From the hysteresis loops of each sample, the related magnetic data including saturation magnetization (Ms), remnant magnetization (Mr), positive Mr, negative Mr and coercivity (Hci) values were extracted and inserted in caption of Figs. 5a-c. The obtained magnetic values for the prepared MIONs are as follow:

For glucose capped MIONs: Ms=42.69 emu g^{-1}, Mr=0.34 emu g^{-1}, positive Mr=0.25 emu g^{-1}, negative Mr=-0.44 emu g^{-1} and Hci=8.39 G. For sucrose coated MIONs: Ms=31.86 emu g^{-1}, Mr=0.07 emu g^{-1}, positive Mr=0.21 emu g^{-1}, negative Mr=0.35 emu g^{-1} and Hci=2.29 G. And for starch capped MIONs, Ms=23.51 emu g^{-1}, Mr=0.13 emu g^{-1}, positive Mr=0.06 emu g^{-1}, negative Mr=0.33 emu g^{-1} and Hci=6.31 G. The Ms and Mr values of these samples proved their superparamagnetic nature. All the prepared MIONs exhibited negligible remnant magnetization value, which established their suitability for biomedical application like as hyperemia. Furthermore, these magnetization abilities are comparable with those reported in literature for naked and saccharide coated iron oxide NPs (i.e. IONs) and also Mn doped IONs. For the bare IONs [70,71], it has been reported that the electrochemically synthesized iron oxide NPs are capable to present magnetic capabilities of *Ms*=72.96 emu g^{-1}, *Mr*=0.95 emu g^{-1}, positive *Mr*=2.73 emu g^{-1}. For meal ion doped magnetite NPs (i.e. naked Mn^{2+} doped IONs [61]), it has been observed that the magnetic values are *Ms* =47.25 emu g^{-1}, *Mr*=0.22 emu g^{-1}, positive *Mr*=-0.703 emu g^{-1}, negative *Mr*=-1.15 emu g^{-1}, H_{Ci}=4.84 G, positive H_{Ci}=25.55 and negative H_{Ci}=15.85 G. For the polysaccharide (i.e. glucose, fructose and sucrose) coated superparamagnetic iron oxide nanoparticles (SPIONs) prepared by co-precipitation method [62], the following magnetic data have been reported: For glucose coated SPIONs, *Ms*=41.69 emu g^{-1}, *Hci* =0.55 Oe, For fructose coated SPIONs; *Ms*=38.43 emu g^{-1}, *Hci*=4.42 Oe and for sucrose coated SPIONs, *Ms*=42 emu g^{-1}, *Hci*=9.13 Oe [62].

Also, Sari *et al.* reported the saturation magnetization and coercively values of *Ms*=35.41 emu g^{-1}, *Hci*=83.58 Oe, for glucose coated IONs, [67]. Comparing these data indicated that our prepared samples have smaller *Hci* and Mr values and better magnetic nature.

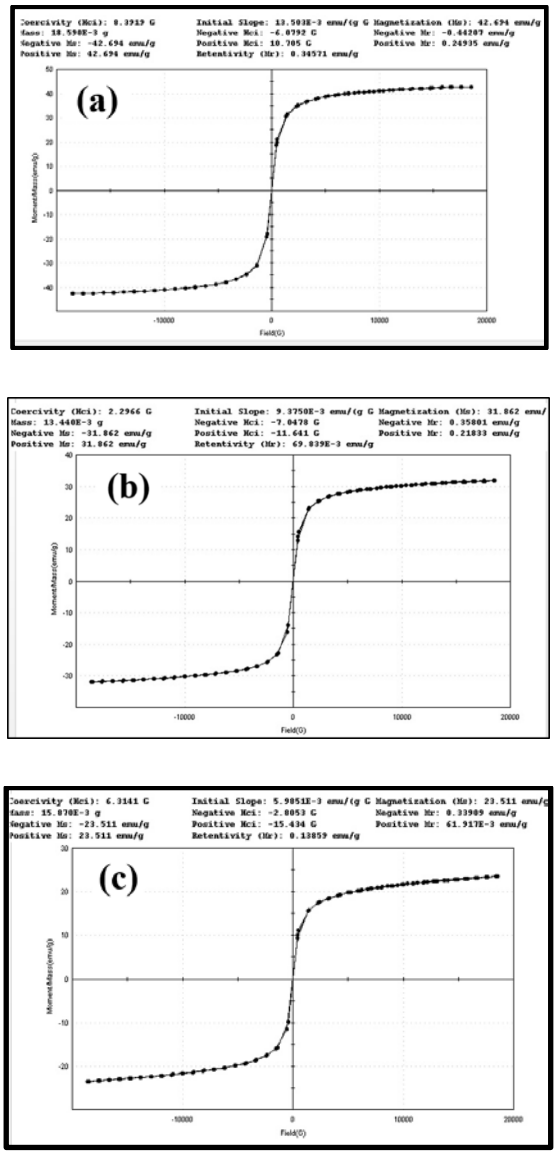

Fig. 5. Room temperature M-H curves for the electrochemically fabricated (a) glucose-MIONs; (b) sucrose-MIONs and (c) Starch-MIONs samples

4. CONCLUSION

In summary, metal cation doped iron oxide nanoparticles capped with saccharides (glucose, sucrose and starch) was synthesized through an electrochemical method. The average nanocrystallite size were found to be 7.8 nm, 9.8 nm and 7.4 nm from powder XRD and the average particle diameter obtained from FE-SEM provides a value 20 nm, 30 nm and 25 nm for glucose-MIONs, sucrose-MIONs and starch-MIONs, respectively. The VSM

results indicated that the prepared sample exhibit superparamagnetic behavior and have proper magnetic capability for possible biomedical applications.

REFERENCES

[1] Y. Hu, S. Mignani, J. P. Majoral, M. Shen, and X. Shi, Chem. Soc. Rev. 47 (2018) 1874.

[2] S. Laurent, D. Forge, M. Port, A. Roch, C. Robic, L. Vander Elst, and R. N. Muller, Chem. Rev. 108 (2008) 2064.

[3] J. Gao, H. Gu, and B. Xu, Acc. Chem. Res. 42 (2009) 1097.

[4] A. Feld, R. Koll, L. S. Fruhner, M. Krutyeva, W. Pyckhout-Hintzen, C. Wei, H. Heller, A. Weimer, C. Schmidtke, M. S. Appavou, E. Kentzinger, J. Allgaier, and H. Weller, ACS Nano 11 (2017) 3767.

[5] T. Javanbakht, S. Laurent, D. Stanicki, and K. J. Wilkinson, PLoS ONE 11 (2016) e0154445.

[6] D. Mousavi, F. Maghsoodi, F. Panahandeh, R. Yazdian-Robati, A. Reisi-Vanani, and M. Tafaghodi, Mater. Sci. Eng. C (2018) In Press.

[7] E. Amstad,a M. Textora, and E. Reimhult, Nanoscale 3 (2011) 2819.

[8] R. Qiao, C. Yang, and M. Gao, J. Mater. Chem. 19 (2009) 6274.

[9] Y. Wang, C. Xu, Y. Chang, L. Zhao, K. Zhang, Y. Zhao, F. Gao, and X. Gao, ACS Appl. Mater. Interfaces 9 (2017) 28959.

[10] H. Li Chee, C. Ruey R. Gan, M. Ng, L. Low, D. G. Fernig, K. K. Bhakoo, and D. Paramelle, ACS Nano, Article ASAP (2018) 07572.

[11] S. K. Mishra, S. Khushu, and A. K. Singh, Stem Cell Rev and Rep (2018) doi:0.1007/s12015-018-9828-7

[12] G. Kandasamy, A. Sudame, T. Luthra, K. Saini, and D. Maity, ACS Omega 3 (2018) 3991.

[13] T. Eslaminejad, S. N. Nematollahi-Mahani, and M. Ansari, Curr. Gene Therapy 17 (2017) 59.

[14] S. Moise, E. Céspedes, D. Soukup, J. M. Byrne, Alicia J. El Haj, and N. D. Telling, Scientific Reports 7 (2017) 39922.

[15] G. Cordova, S. Attwood, R. Gaikwad, F. Gu, and Z. Leonenko, Nano Biomed Eng. 6 (2014) 31.

[16] M. M. Lin, H. H. Kim, H. Kim, J. Dobson, and D. K. Kim, Nanomed. 5 (2010) 109.

[17] R. Serrano García, S. Stafford, and Y. K. Gunko, Appl. Sci. 8 (2018) 172.

[18] A. S. Fortuin, R. Brüggemann, J. van der Linden, I. Panfilov, B. Israël, T. W. J. Scheenen, and J. O. Barentsz, WIREs Nanomed. Nanobiotechnol. 10 (2018) e1471.

[19] J. Ding, J. Zhao, K. Cheng, G. Liu, and D. Xiu, J. Biomed. Nanotechnol. 6 (2010) 683.

[20] P. O. Champagne, H. Westwick, A. Bouthillier, and M. Sawan, Nanomedicine 13 (2018) 1385.
[21] X. C. Zheng, W. Ren, S. Zhang, T. Zhong, X. C. Duan, Y. F. Yin, and M. Q. Xu, Int. J. Nanomed. 13 (2018) 1495.
[22] A. Ali, H. Zafar, M. Zia, I. Ul Haq, A. R. Phull, J. S. Ali, and A. Hussain, Sci. Appl. 9 (2016) 49.
[23] S. Razzaque, S. Z. Hussain, I. Hussain, and B. Tan, Polymers 8 (2016) 156.
[24] Kai Li, H. Nejadnik, and H. E. Daldrup-Link, Drug Discovery Today 22 (2017) 1421.
[25] B. M. Geilich, I. Gelfat, S. Sridhar, A. L. van de Ven, and T. J. Webster, Biomaterial 119 (2017) 78.
[26] A. R. Nochehdehi, S. Thomas, M. Sadri, S. S. S. Afghahi, and S. M. Mehdi Hadavi, J. Nanomed. Nanotechnol. 8 (2017) 1.
[27] W. Wu, Q. He, and C. Jiang, Nanoscale Res. Lett. 3 (2008) 397.
[28] P. Majewski, and B. Thierry, Critical Rev. Solid State Mater. Sci. 32 (2007) 203.
[29] C. Boyer, M. R. Whittaker, V. Bulmus, J. Liu, and T. P. Davis, NPG Asia Mater. 2 (2010) 23.
[30] R. Alwi, S. Telenkov, A. Mandelis, T. Leshuk, F. Gu, S. Oladepo, and K. Michaelian, Biomed. Opt. Express. 3 (2012) 2500.
[31] M. Mahmoudi, and V. Serpooshan, ACS Nano 6 (2012) 2656.
[32] M. Aghazadeh, and I. Karimzadeh, Curr. Nanosci. 14 (2018) 42.
[33] M. Aghazadeh, I. Karimzadeh, and M. R. Ganjali, Mater. Lett. 228 (2018) 137.
[34] I. Karimzadeh, M. Aghazadeh, M. R. Ganjali, P. Norouzi, S. Shirvani-Arani, T. Doroudi, P. H. kolivand, S. A. Marashi, and D. Gharailou, Mater. Lett. 179 (2016) 5.
[35] I. Karimzadeh, M. Aghazadeh, M. R. Ganjali, and T. Dourudi, Curr. Nanosci. 13 (2017) 167.
[36] I. Karimzadeh, H. Rezagolipour Dizaji, and M. Aghazadeh, Mater. Res. Express. 3 (2016) 095022.
[37] I. Karimzadeh, H. R. Dizaji, and M. Aghazadeh, J. Magn. Magn. Mater. 416 (2016) 81.
[38] M. Bloemen, W. Brullot, T. Thien, L. Nick, G. Ann, and G. Thierry Verbiest, J. Nanopart. Res. 14 (2012) 1100
[39] J. Castello, M. Gallardo, M. Antonia Busquets, and J. Estelrich, Colloids Surf. A 468 (2015) 151.
[40] M. Aghazadeh, I. Karimzadeh, and M. R. Ganjali, J. Electronic Mater. 47 (2018) 3026.
[41] M. Aghazadeh, and M. R. Ganjali, J. Mater. Sci.: Mater. Electron. 29 (2018) 4981.
[42] M. Aghazadeh, Mater. Lett. 211 (2018) 225.
[43] M. Aghazadeh, and M. R. Ganjali, Ceram. Int. 44 (2018) 520.
[44] M. Aghazadeh, M. G. Maragheh, M. R. Ganjali, and P. Norouzi, Inorg. Nano-Metal Chem. 27 (2017) 1085.

[45] M. Aghazadeh, J. Mater. Sci.: Mater. Electron. 28 (2016) 3108.
[46] M. Aghazadeh, M. G. Maragheh, M. R. Ganjali, and P. Norouzi, RSC Adv. 6 (2016) 10442.
[47] M. Aghazadeh, A. Nozad, H. Adelkhani, and M. Ghaemi, J. Electrochem. Soc. 157 (2010) D519.
[48] M. Aghazadeh, M. Ghaemi, A. N. Golikand, and A. Ahmadi, Mater. Lett. 65 (2011) 2545.
[49] M. Aghazadeh, A. A. M. Barmi, H. M. Shiri, and S. Sedaghat, Ceram. Int. 39 (2013) 1045.
[50] M. Aghazadeh, A. A. M. Barmi, and M. Hosseinifard, Mater. Lett. 73 (2012) 28.
[51] M. Aghazadeh, and M. R. Ganjali, J. Mater. Sci.: Mater Electron. 28 (2017) 8144.
[52] V. A. J. Silva, P. L. Andrade, M. P. C. Silva, A. Bustamante Dominguez, L. S. Valladares, and J. A. Aguiar, J. Magn. Magn. Mater. 343 (2013) 138.
[53] Mutasim I. Khalil, Arabian J. Chem. 8 (2015) 279.
[54] A. L. Andrade, M. A. Valente, J. M. F. Ferreira, and J. D. Fabris, J. Magn. Magn. Mater. 324 (2012) 1753.
[55] M. Aghazadeh, and I. Karimzadeh, Mater. Res. Express 4 (2017)105505.
[56] M Aghazadeh, J. Mater. Sci.: Mater. Electron. 28 (2017) 18755.
[57] M. Aghazadeh, I. Karimzadeh, M. Ghannadi Maragheh, and M. R. Ganajli, Korean J. Chem. Engin. 35 (2018) 1341.
[58] M. Aghazadeh, and M. R. Ganjali, J. Mater. Sci. 53 (2018) 295.
[59] M. Aghazadeh, I. Karimzadeh, and M. R. Ganjali, J. Mater. Sci.: Mater. Electron. 28 (2017) 19061
[60] M. Aghazadeh, I. Karimzadeh, and M. R. Ganjali, J. Mater. Sci.: Mater. Electron. 28 (2017) 13532
[61] M. Aghazadeh, I. Karimzadeh, M. R. Ganjali, and A. Behzad, J. Mater. Sci.: Mater. Electron. 28 (2017) 18121.
[62] D. Sivakumar, M. M. Rafi, B. Sathyaseelan, K. M. Prem Nazeer, and A. M. Ayisha Begam, Int. J. Nano Dimens. 8 (2017) 257.
[63] I. Karimzadeh, M. Aghazadeh, T. Doroudi, M. R. Ganjali, P. H. Kolivand, and D. Gharailou, Curr. Nanosci. 13 (2017) 274.
[64] A. Demir, A. Baykal, and H. Sozer, Turk. J. Chem. 38 (2014) 825.
[65] I. Karimzadeh, M. Aghazadeh, M. R. Ganjali, P. Norouzi, T. Doroudi, and P. H. Kolivand, Mater. Lett. 189 (2017) 290.
[66] M. Aghazadeh, I. Karimzadeh, M. R. Ganjali, and M. Mohebi Morad, Mater. Lett. 196 (2017) 392.
[67] A. Y. Sar, A. S. Eko, K. Candra, D. P. Hasibuan, M. Ginting, P. Sebayang, and P. Simamora, IOP Conf. Series: Mater. Sci. Eng. 214 (2017) 012021.

[68] A. B. Brizuela, L. C. Bichara, E. Romano, A. Yurquina, S. Locatelli, and S. A. Brandán, Carbohydrate Res. 361 (2012) 212.
[69] W. Lu, Y. Shen, A. Xie, and W. Zhan, J. Phys. Chem. B 117 (2013) 3720.
[70] M. Aghazadeh, and M. R. Ganjali, J. Mater. Sci.: Mater. Electron. 29 (2018) 2291.
[71] M. Aghazadeh, I. Karimzadeh, and M.R. Ganjali,Mater. Res. 21 (2018) e20180094.